Towards a Realistic Surface State of Ru in Aqueous and Gaseous Environments

Muhammad Akif Ramzan, Raphaël Wischert, Stephan N. Steinmann, Carine Michel

Towards a Realistic Surface State of Ru in Aqueous and Gaseous Environments

Muhammad Akif Ramzan,[†] Raphaël Wischert,[‡,¶] Stephan N. Steinmann,[†] and Carine Michel[*,†]

†*ENS de Lyon, CNRS UMR 5182, Laboratoire de Chimie, F69342, Lyon, France*

‡*Eco-Efficient Products and Processes Laboratory (E2P2L), UMI 3464 CNRS-Solvay, 3966 Jin Du Road, Xin Zhuang Ind. Zone, 201108 Shanghai, China*

¶*Current address: Solvay Lyon Research and Innovation Center, 85 Av. des Frères Perret, 69190 Saint-Fons, France*

E-mail: carine.michel@ens-lyon.fr

Abstract

Identifying the surface species is critical towards a realistic understanding of supported metal catalysts working in water. To this end, we have characterized the surface species present at a Ru/water interface by employing a hybrid computational approach involving an explicit description of the liquid water and a possible pressure of H_2. On close-packed, most stable Ru(0001) facet, the solvation tends to favor the full dissociation of water into atomic O and H in contrast with the partially-dissociated water layer reported for ultra-high vacuum conditions. The solvation stabilization was found to be as high as -0.279 J.m^2 which results in stable O and H species on Ru(0001) in presence of liquid water even at room temperature. Conversely, introducing even a small H_2 pressure (10^{-2} bar) results in a monolayer of chemisorbed H at the interface, a general trend found on the three most exposed facets of Ru nanoparticles. While hydroxyls were often hypothesized as possible surface species at the Ru/water interface, this computational study clearly demonstrates that they are not stabilized by liquid water and are not found in realistic reductive catalytic conditions.

TOC Graphic

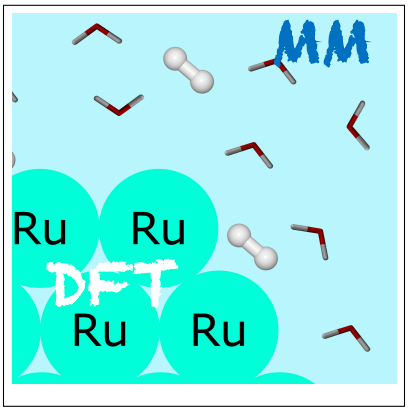

The Ru/water interface has been extensively studied as a prototypical system to understand the interaction of water with metals.[1–7] Using first principles calculations, Feibelman showed that the wetting layer on Ru(0001) was not a water bilayer analogous to those forming ice-Ih, but rather a partially-dissociated layer comprising H_2O/OH hexagonal patterns with H atoms occupying the empty top sites.[8] This structure was more stable and in better agreement with previous LEED structural analysis by Held and Menzel.[9] Revisiting the thermal desorption of water on Ru(0001), Denzler et al. confirmed the dissociative adsorption, at least for a small amount of water.[10] Michaelides et al. showed that the barrier to break the O-H bond on Ru(0001) was 50 kJ·mol^{-1}within the water bilayer vs. 80 kJ·mol^{-1} found for an isolated water molecule.[11] Still, water dissociation was shown to be an activated process, with a barrier sligthly larger than water desorption.[12] More recently, Schilling et al. used STM experiments to highlight that this dissociation is thermally induced around 100-120 K.[13] In summary, the formation of the partially-dissociated water layer on Ru(0001) is now a well-established phenomenon above 120 K in ultra high vacuum conditions.

These surface science studies put forward the possible formation of $Ru(OH)_x$ species on supported-Ru nanoparticles in water. The presence and, in turn, the potential influence of these hydroxyl species is, however, controversial as they were hypothesized to account for both the catalyst deactivation observed for hydrogenation of butan-2-one in water[14] as well as the remarkable efficiency of supported-Ru catalysts to hydrogenate carbonyl compounds in aqueous phase.[15] This enhanced efficiency of supported-Ru catalysts for hydrogenation of carbonyl compounds in water was alternatively explained in terms of a solvation effect involving interaction of adsorbed H_2O species with the reaction intermediates.[16,17] This solvation effect was also observed for the reverse water gas shift reaction catalyzed by Ru where CO_2 is reduced into CO by a pressure of H_2.[18] Moreover, the partially-dissociated surface water on Ru(0001) was shown to be surprisingly acidic using NH_3 as a probe molecule.[19] In short, identifying the species exposed at the Ru/water interface appears critical to better rationalize the unique ability of Ru to perform catalysis in water.

The stability of hydroxyl group at the Ru/water interface is likely strongly influenced by the presence of liquid water, the temperature (400-500 K) and the possible presence of H_2 (0-50 bar). In stark contrast, surface science studies are performed under ultra-vacuum conditions at low temperatures. Bridging the gap to more realistic reaction conditions of temperature and pressure is needed, including conditions where water is liquid. A first attempt in that direction was the study by Messaoudi *et al.*,[20] who investigated computationally the effect of a second water layer on the relative stability of intact and partially-dissociated (mono-)layer on Ru(0001). They found that the wetting by second layer is more favorable for the partially-dissociated layer than for the intact one. Using ab initio molecular dynamics, water molecules were found to dissociate at 300 K at the interface between Ru(0001) and a slab of liquid water,[7] in contrast with Pt and Pd where the water molecules stay intact. On the other hand, under oxidative (electro-)catalytic conditions, water dissociation is not only observed over Ru, but over most metals.[6,21,22] Still, the effects of temperature and a pressure of H_2 were not included, and the influence of solvation by liquid water will likely differ from a frozen water layer. To tackle this issue, we propose here to extend DFT-based *ab initio* atomistic thermodynamics (AITD) to the identification of surface species at the metal/water interface. AITD is a well-established technique to study the relative stability of a solid phase in contact with a gas phase environment at specified temperature and pressure.[23] To achieve a more accurate description of solvation phenomena, we complement the AITD model with solvation energies obtained by a QM/MM model developed by some of us.[24]

We have focused on the three most-exposed Ru facets based on a Wulff construction in the gas-phase, namely Ru(0001) (16%), Ru(10$\bar{1}$0) (21%) and Ru(10$\bar{1}$1) (43%).[25] To identify the surfaces species when these facets are in contact with water and/or H_2, we have applied the following methodology:

1. Generate configurations exposing a mixture of H, O, OH and H_2O on each facet using symmetric slab model;

2. Optimize and extract their relative stability at the GGA-PBE level including a density-dependent dispersion correction (dDsC);[26,27]

3. Compute the relative Gibbs free energy using AITD to include the effect of the environment (H_2, H_2O). When water is considered as liquid, a solvation term ΔG_{solv} is added to the relative Gibbs free energy (see below).

To generate the collection of configurations, we first identified the distinct adsorption sites available on the surface of each facet (see Fig. S3). We then calculated the adsorption strength of different isolated species on each surface (see Table S3). Subsequently, based on the preferred type of adsorption site (fcc, hcp etc.) we generated a database of the surface configurations for the three facets by random placement of the adsorbates on suitable surface sites (more details in Supporting Information (SI)). In addition to the random configurations, the adsorption of O and H atoms was systematically studied at each level of coverage for all three facets. The intact and partially-dissociated water layers on Ru(0001)[8] were also included in the data set. In total, this database included 316 structures on Ru(0001), 261 on Ru($10\bar{1}0$) and 311 on Ru($10\bar{1}1$) . The correction term for solvation (ΔG_{solv}) was added to at least 100 most stable configurations on each facet.

As a first case, we consider the Ru(0001)/water interface in absence of H_2 (or any other source of O and H) and with or without solvation. The subcase without solvation amounts to water being in vapor phase and has been extensively studied using surface science[9,10,13,28] and DFT.[8,11,20] Notably, this condition limits the surface configurations to only those with an O:H ratio of 1:2; and the stability of a given configuration relative to a reference is given by,

$$\Delta G_{ads}\left(T\right) = \frac{1}{2A}\left[G - G_{ref} - \Delta n_{\mathrm{H_2O}} \mu_{\mathrm{H_2O}}\left(T\right) + \Delta G_{solv}\right] \tag{1}$$

where A is the area of the slab supercell; G is the Gibbs energy of this configuration; G_{ref} is the Gibbs energy of a potentially arbitrary reference configuration on the same facet, on Ru(0001) e.g. it was taken to be the partially-dissociated water monolayer proposed by

Fiebelmann;[8] Δn_{H_2O} is the number of water molecules to fulfill the stoichiometry between reference and given configuration and μ_{H_2O} is the chemical potential of water that is fixed by the experimental saturation vapor pressure of water which, in turn, is fixed by the temperature, the only thermodynamic parameter required for this case. The solvation term ΔG_{solv} is computed using our MMSolv scheme[24] as the *difference* in solvation energies between the reference and the targeted configuration. Computationally, this was achieved at MM level by implementing an alchemical transformation between the two configurations based on thermodynamic integration. In the remaining text, this quantity is reported for a symmetric slab in kJ·mol^{-1}and/or in J.m^{-2}. More details on MMSolv scheme are provided in the SI.

In Figure 1 we report ΔG_{ads} as a function of temperature with (right) and without (left) solvation along with the top view of the most stable phases for Ru(0001) based on 111 configurations in our dataset that have the required O:H ratio. For the familiar subcase with no solvation, below $\sim$ 340 K, the most stable phase is the partially-dissociated monolayer of water, consistent with previous studies.[8,10] Above this temperature the most stable phase was found to be a configuration with two water molecules fully dissociated and O and H both binding to hcp hollow sites. Surprisingly, configurations with OH species do not appear in the stability plot above 340 K and a full dissociation of water is thermodynamically preferred. This can be rationalized based on the tendency of water to easily split on Ru(0001) and the entropic gain achieved by more water being in the vapor phase as the temperature increases. When solvation is invoked to better mimic the solid/liquid interfaces found in heterogeneous catalysis, the fully-dissociated configuration is the most stable at all temperatures, which can be attributed to its strongly stabilizing solvation free energy (ΔG_{solv}= -191 kJ·mol^{-1}= -0.279 J.m^{-2}). Similar behavior was observed on other two facets considered in this study. In summary, this result indicates that water is prone to full dissociation at the Ru(0001) surface and that this dissociation is enhanced by solvation i.e. the presence of liquid water.

Now, we move to the situation where the Ru surfaces are in contact not only with water but also H_2. This allows relaxing the constraint of O:H ratio required for previous

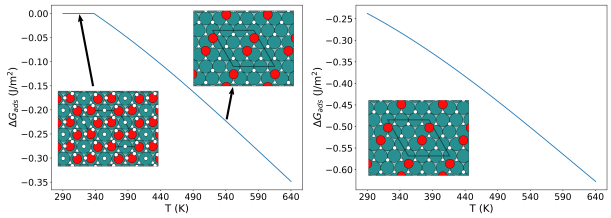

Figure 1: Adsorption free energy as a function of temperature in (left) water as a vapor at saturation pressure and (right) water as liquid in equilibrium with its vapor on Ru(0001). The value at each temperature corresponds to the most stable phase which are shown on the plot. ΔG_{ads} value of 0 corresponds to the reference state which is the partially-dissociated water layer shown on left plot.

case and all possible combinations of H/O/OH/H_2O could potentially occur on the surface. Consequently, Eq. 1 can be generalized as:

$$\Delta G_{ads}\left(T,p\right) = \frac{1}{2A}\left[G - G_{ref} - \Delta n_H \mu_H\left(T,p\right) - \Delta n_O \mu_O\left(T,p\right) + \Delta G_{solv}\right] \tag{2}$$

where $\mu_H\left(T,p\right)$ is the chemical potential of H controlled by the pressure of H_2 and temperature; $\mu_O\left(T,p\right)$ is the chemical potential of O controlled by the chemical potential of $\mu_{H_2O}\left(T\right)$ *via* $\mu_{H_2O}\left(T\right) = \mu_{H_2}\left(T,p\right) + \mu_O\left(T,p\right)$, which is valid at thermodynamic equilibrium. Notably, introduction of H_2 introduces another thermodynamic parameter and the 2-dimensional phase space is now defined by temperature and pressure of H_2.

Figures 2, 3 and S4 show the most stable adsorption configurations and the corresponding stability domains for Ru(10$\bar{1}$0), Ru(0001) and Ru(10$\bar{1}$1), respectively. We report the stability map without and with the solvation contribution ΔG_{solv} to contrast two cases: (i) water as a vapor at saturation pressure, (ii) water as liquid in equilibrium with its vapor. The first case can also be seen as a solid/liquid interface model including only the first layer in contact with the solid.

On all three surfaces, the presence of a pressure of H_2 above 10^{-2} bar is enough to cause a monolayer of H in the whole range of temperature (290-640 K), independently of the treatment of water (as vapor at the saturation pressure or as liquid). The second most stable surface topology at lower p_{H_2} depends on the type of facet. On the most exposed

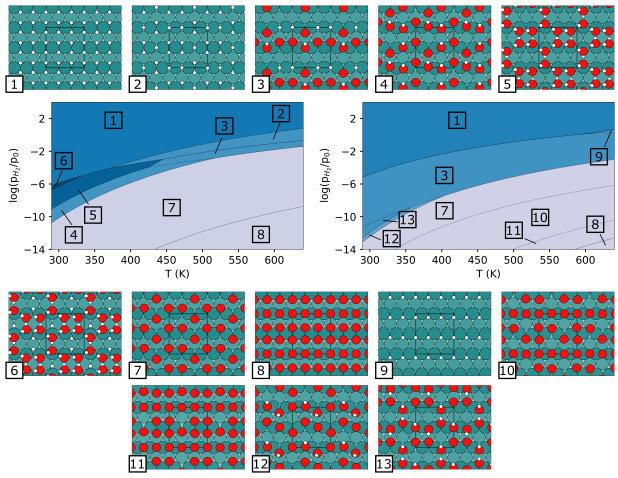

Figure 2: The most stable adsorption geometries of H_2O/OH/O/H on Ru(10$\bar{1}$0) exposed to a pressure of H_2 and the corresponding T-p maps displaying the stability of different adsorption phases in (left) water as vapor at saturation pressure and (right) water as a liquid in equilibrium with its vapor.

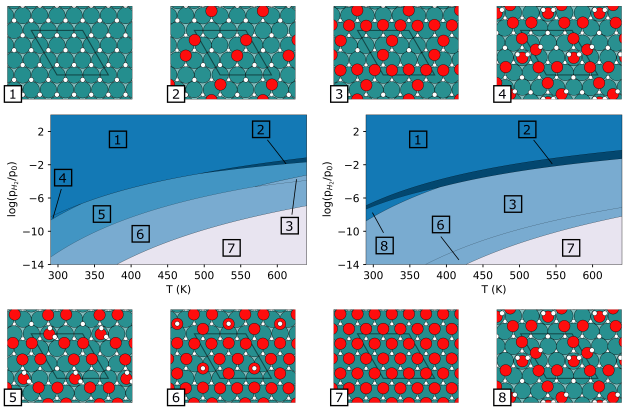

Figure 3: The most stable adsorption geometries of H_2O/OH/O/H on Ru(0001) exposed to a pressure of H_2 and the corresponding T-p maps displaying the stability of different adsorption phases in (left) water as vapor at saturation pressure and (right) water as a liquid in equilibrium with its vapor.

facet Ru($10\bar{1}1$), the monolayer of H switches suddenly to a monolayer of O (Figure S4). Including solvation by liquid water does not change this behavior and only increases the stability domain of the O monolayer due to a greater stabilisation (the O monolayer is more stabilized than the H monolayer by 0.323 J.m^{-2}, see Table S4). On the second most exposed facet Ru($10\bar{1}0$), OH groups can be found in a variety of O/H/H_2O environments (as in **3-6** and **12-13**). Interestingly, the stability domain of **3**, which is constituted of OH, O and H, increases upon solvation at the expense of H-covered configurations (**1** and **2**) but also a O-covered structure (**7**). This can be directly related to the greater stabilisation by solvation of **3** relative to the others (by at least 0.143 J.m^{-2}, see Table S5). Lastly, on the most stable Ru(0001) facet, the second best configuration (**5**) includes not only O and H but also OH and H_2O. It is replaced by **2** and **3** upon inclusion of solvation, a configuration that includes only O and H, confirming again that liquid water is more susceptible to full dissociation than saturated water vapor on Ru(0001). In short, supported-Ru nanoparticles exposed to water would be mainly covered by H and exhibit hydroxyl groups on Ru($10\bar{1}0$) and O species on the other two facets . However, the OH and O concentration will be considerably reduced by the presence of a pressure of hydrogen (above 0.1 bar at 500 K).

To better understand how the presence of liquid water modifies the Ru/water interface, we further investigated the variation in solvation between typical configurations on the three facets considered.[24] To start, we studied thermodynamic cycles (Figure 4) for typical adsorption structures on all three facets to validate the MMSolv scheme. We found that the MMSolv approach is self-consistent (the sum of the values along horizontal arrows is equal to the value along the curved arrow) within a small 2 kJ·mol^{-1}error, demonstrating satisfactory convergence of the results. Noticeably, the monolayer of H_2O is systematically less solvated than a monolayer of H or a monolayer of O on all three surfaces. The biggest change in solvation (ΔG_{solv} = -177 kJ.mol^{-1}) is observed when going from H_2O-Ru($10\bar{1}1$) to H-Ru($10\bar{1}1$) . In other words, two chemisorbed H are better solvated than one chemisorbed water molecule by $\sim$ 15 kJ·mol^{-1}. At first sight, this is rather counter-intuitive since more

interactions (hydrogen bonding) are expected between liquid water and chemisorbed water than between liquid water and a monolayer of H. However, changes in water structuring at the interface can also be responsible for the observed variation in solvation.

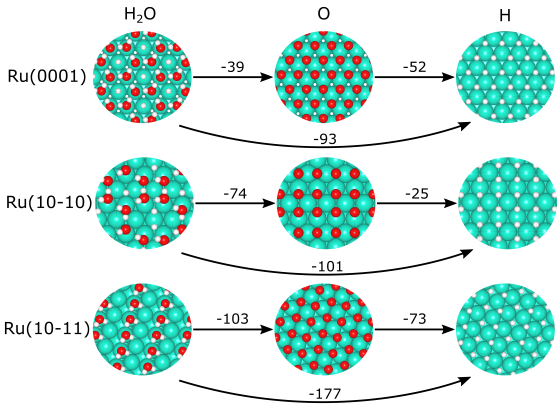

Figure 4: Error assessement of the MMSolv approach. The values are ΔG_{solv} in kJ.mol^{-1}.

To understand these unexpected effects of solvation, we analyzed the structure of MM water above the Ru(0001)-adsorbate surface. First, we looked at the distribution of O-WAT and H-WAT atoms present in liquid MM water as a function of distance from the metallic surface. The corresponding graphs are given in Figure S5 for H_2O-Ru(0001), H-Ru(0001), O-Ru(0001) and the configuration **2** that was found to be stabilized by solvation (see Figure 3). This configuration contains two fully dissociated water molecules and is tagged O-H-Ru(0001) in the remaining text. Looking at the shape of the distribution curves, one immediately sees that they all converge to 1 for O-WAT, 2 for H-WAT far from the surface, which is the expected bulk-like behavior. Secondly, all the curves involve a first peak which shows an accumulation of the water at the interface and can be characterized by the distance at which O-WAT shows highest value (x_{peak}). An estimate of the number of water molecules in the first layer, N_{H_2O}, is obtained by calculating the area under this first peak. These numbers, along with ΔG_{solv} values, have been tabulated in Table 1. As shown in Table S7, these quantities are not sensitive to the charge rescaling in the MMSolv calculations.

In the reference interface (H_2O-Ru(0001)), the first layer is dense, containing 8.8 molecules in a p(3x3) supercell and the density of O-WAT peaks at 5.17 Å. For the three other in-

terfaces, which are better solvated, the first layer contains less water molecules than the reference interface. However, a lower x_{peak} found on those interfaces could account for a more favorable ΔG_{solv}, indicating that the localisation of the hydration layer is key to the strength of solvation of adsorbate-modified Ru surfaces. The variation in solvation from O-Ru(0001) to H-Ru(0001), two starkly different interfaces, could be rationalized based on two effects: (i) the smaller size of H allows water to approach closer to the surface, as indicated by the smaller x_{peak} value, which establishes a stronger H_2O/Ru interaction resulting in higher solvation (ii) high polarity of O-Ru(0001) surface induces undesirable structuring of water over this interface which results in loss of solvation compared to H-Ru(0001). The mixed O-H-Ru(0001) configuration has the highest free energy change of solvation, more than that of H-Ru(0001) and O-Ru(0001) combined. Noticeably, this behavior was also observed for other similar configurations with mixed O and H species on the surface. We suspect that the O and H species on the surface act in a synergistic fashion to draw MM water molecules closer to the surface in localized pockets (evidenced by the lowest x_{peak} value) leading to a higher solvation. In particular, some water molecules can approach the surface very closely above the H-covered zone to engage in hydrogen bonding with the surface O atoms. A typical configuration is represented in Figure 5 where the hydrogen bonds are highlighted using red dashed line (O...O <3Å, $\measuredangle OOH$<20°).

Table 1: Position of the first density peak x_{peak}, number of H_2O molecules in the first layer above the surface calculated as the integral of first peak in the graphs given in Figure S5 and the corresponding solvation enthalpy change for four adsorption configurations of Ru(0001).

Configuration	x_{peak} (Å)	N_{H_2O}	Dipole (e.Å)	ΔG_{solv} (kJ.mol^{-1})	(J.m^{-2})
H_2O-Ru(0001) - **Ref.**	5.03	8.8	-0.07	0	0
O-Ru(0001) - **7**	3.67	7.4	0.50	-39	-0.056
H-Ru(0001) - **1**	3.34	6.6	-0.03	-93	-0.135
O-H-Ru(0001) - **2**	2.74	6.8	0.14	-191	-0.279

In conclusion, we have studied the nature of surface species exposed at the Ru/water interface as a function of the experimental conditions (liquid water, temperature, pressure of

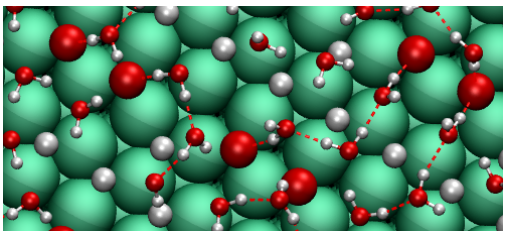

Figure 5: Representative snapshot of the O-H-Ru(0001)/water interface. Ru is shown in green, O and H are shown in red and white, water molecules are shown using a ball-and-stick representation, hydrogen bonds are highlighted using red dashed line (O...O<3Å, $\measuredangle OOH$<20°, which corresponds to the default definition in VMD.)

H_2) using computations. On three separate, most abundant facets of a typical Ru nanoparticle, we find a H monolayer being the most stable adsorption topology in presence of a pressure of H_2 above 10^{-2} bar in the whole temperature range of 290-640 K, independently of the treatment of water (as vapor at the saturation pressure or as liquid). All surface terminations, however, are prone to a partial or full oxidation at high temperatures if little or no H_2 pressure is supplied, exposing O and OH. Interestingly, liquid water favors the presence of some surface OH on Ru(10$\bar{1}$0) , the second most exposed facet. Even if those species are not the most exposed species, they may be exposed in large enough quantity to affect a catalytic process. Importantly, liquid water is more prone to full dissociation than expected based on surface science studies due to stabilisation of configurations mixing O and H vs. mixing OH and H_2O species on the surface.

Supporting Information Available

Computationnal details ; Thermodynamic formalism ; Ab initio data on single atom/molecule adsorption used in the random phase generator ; complementary data on solvation.

The authors express their gratitude to Solvay for funding. This work has been realized with the financial support of the IDEXLYON project of the Université de Lyon in the framework of the Projet d'Investissement d'Avenir (ANR-16-IDEX-0005), as well as the SYSPROD and Axelera Pole de Competitivite (PSMN Data Center). This study also received granted

access to the HPC resources of the CINES and IDRIS under the allocation 0800609 made by the GENCI.

References

(1) Gallagher, M.; Omer, A.; Darling, G. R.; Hodgson, A. Order and disorder in the wetting layer on Ru(0001). *Faraday Discussions* **2008**, *141*, 231–249.

(2) Hodgson, A.; Haq, S. Water adsorption and the wetting of metal surfaces. *Surface Science Reports* **2009**, *64*, 381–451.

(3) Tatarkhanov, M.; Ogletree, D. F.; Rose, F.; Mitsui, T.; Fomin, E.; Maier, S.; Rose, M.; Cerdá, J. I.; Salmeron, M. Metal- and Hydrogen-Bonding Competition during Water Adsorption on Pd(111) and Ru(0001). *Journal of the American Chemical Society* **2009**, *131*, 18425–18434.

(4) Li, X.-Z.; Probert, M. I. J.; Alavi, A.; Michaelides, A. Quantum Nature of the Proton in Water-Hydroxyl Overlayers on Metal Surfaces. *Physical Review Letters* **2010**, *104*, 066102.

(5) Carrasco, J.; Santra, B.; Klimeš, J.; Michaelides, A. To Wet or Not to Wet? Dispersion Forces Tip the Balance for Water Ice on Metals. *Physical Review Letters* **2011**, *106*, 026101, Publisher: American Physical Society.

(6) Björneholm, O.; Hansen, M. H.; Hodgson, A.; Liu, L.-M.; Limmer, D. T.; Michaelides, A.; Pedevilla, P.; Rossmeisl, J.; Shen, H.; Tocci, G. et al. Water at Interfaces. *Chemical Reviews* **2016**, *116*, 7698–7726.

(7) Bellarosa, L.; García-Muelas, R.; Revilla-López, G.; López, N. Diversity at the Water–Metal Interface: Metal, Water Thickness, and Confinement Effects. *ACS Central Science* **2016**, *2*, 109–116.

(8) Feibelman, P. J. Partial dissociation of water on Ru(0001). *Science (New York, N.Y.)* **2002**, *295*, 99–102.

(9) Held, G.; Menzel, D. The structure of the p($\sqrt{3} \times \sqrt{3}$)$R30°$ bilayer of D2O on Ru(001). *Surface Science* **1994**, *316*, 92–102.

(10) Denzler, D.; Wagner, S.; Wolf, M.; Ertl, G. Isotope effects in the thermal desorption of water from Ru(001). *Proceedings of the 7th International Conference on Nanometer-Scale Science and Technology and the 21st European Conference on Surface Science* **2003**, *532-535*, 113–119.

(11) Michaelides, A.; Alavi, A.; King, D. A. Different Surface Chemistries of Water on Ru(0001): From Monomer Adsorption to Partially Dissociated Bilayers. *Journal of the American Chemical Society* **2003**, *125*, 2746–2755.

(12) Andersson, K.; Nikitin, A.; Pettersson, L. G. M.; Nilsson, A.; Ogasawara, H. Water Dissociation on Ru(001): An Activated Process. *Physical Review Letters* **2004**, *93*, 196101.

(13) Schilling, M.; Behm, R. J. Partial dissociation of water on Ru(0001) at low temperatures – Adsorption, structure formation and hydrogen passivation effects. *Surface Science* **2018**, *674*, 32–39.

(14) Manyar, H. G.; Weber, D.; Daly, H.; Thompson, J. M.; Rooney, D. W.; Gladden, L. F.; Hugh Stitt, E.; Jose Delgado, J.; Bernal, S.; Hardacre, C. Deactivation and regeneration of ruthenium on silica in the liquid-phase hydrogenation of butan-2-one. *Journal of Catalysis* **2009**, *265*, 80–88.

(15) Michel, C.; Gallezot, P. Why Is Ruthenium an Efficient Catalyst for the Aqueous-Phase Hydrogenation of Biosourced Carbonyl Compounds? *ACS Catalysis* **2015**, *5*, 4130.

(16) Akpa, B.; D'Agostino, C.; Gladden, L.; Hindle, K.; Manyar, H.; McGregor, J.; Li, R.; Neurock, M.; Sinha, N.; Stitt, E. et al. Solvent effects in the hydrogenation of 2-butanone. *Journal of Catalysis* **2012**, *289*, 30–41.

(17) Michel, C.; Zaffran, J.; Ruppert, A. M.; Matras-Michalska, J.; Jędrzejczyk, M.; Grams, J.; Sautet, P. Role of water in metal catalyst performance for ketone hydrogenation: a joint experimental and theoretical study on levulinic acid conversion into gamma-valerolactone. *Chem. Commun.* **2014**, *50*, 12450–12453.

(18) Sathishkumar, N.; Wu, S.-Y.; Chen, H.-T. Mechanistic insights into chemical reduction of CO2 by reverse water-gas shift reaction on Ru(0001) surface: The water promotion effect. *Applied Surface Science* **2022**, *581*, 152354.

(19) Kim, Y.; Moon, E.-s.; Shin, S.; Kang, H. Acidic Water Monolayer on Ruthenium(0001). *Angewandte Chemie International Edition* **2012**, *51*, 12806–12809.

(20) Messaoudi, S.; Dhouib, A.; Abderrabba, M.; Minot, C. Wetting of Intact and Partially Dissociated Water Layer on Ru(0001): a Density Functional Study. *The Journal of Physical Chemistry C* **2011**, *115*, 5834–5840.

(21) Shavorskiy, A.; Gladys, M. J.; Held, G. Chemical composition and reactivity of water on hexagonal Pt-group metal surfaces. *Physical Chemistry Chemical Physics* **2008**, *10*, 6150–6159.

(22) Kristoffersen, H. H.; Vegge, T.; Hansen, H. A. OH formation and H_2 adsorption at the liquid water–Pt(111) interface. *Chemical Science* **2018**, *9*, 6912–6921.

(23) Reuter, K.; Stampfl, C.; Scheffler, M. *Handbook of Materials Modeling, Part A. Methods*; Springer: Berlin, 2005.

(24) Clabaut, P.; Schweitzer, B.; Götz, A. W.; Michel, C.; Steinmann, S. N. Solvation Free Energies and Adsorption Energies at the Metal/Water Interface from Hybrid Quantum-

Mechanical/Molecular Mechanics Simulations. *Journal of Chemical Theory and Computation* **2020**, *16*, 6539–6549.

(25) Tran, R.; Xu, Z.; Radhakrishnan, B.; Winston, D.; Sun, W.; Persson, K. A.; Ong, S. P. Surface energies of elemental crystals. *Scientific data* **2016**, *3*, 160080.

(26) Steinmann, S. N.; Corminboeuf, C. A generalized-gradient approximation exchange hole model for dispersion coefficients. *The Journal of Chemical Physics* **2011**, *134*, 044117.

(27) Gautier, S.; Steinmann, S. N.; Michel, C.; Fleurat-Lessard, P.; Sautet, P. Molecular adsorption at Pt(111). How accurate are DFT functionals? *Phys. Chem. Chem. Phys.* **2015**, *17*, 28921–28930, Publisher: The Royal Society of Chemistry.

(28) Doering, D. L.; Madey, T. E. The adsorption of water on clean and oxygen-dosed Ru(011). *Surface Science* **1982**, *123*, 305–337.